JOURNAL OF CATALYSIS 156, 28–36 (1995)

Evolution of a VPO Catalyst in *n*-Butane Oxidation Reaction during the Activation Time

M. Abon, K. E. Bere, A. Tuel, and P. Delichere

Institut de Recherches sur la Catalyse, CNRS, 2, Avenue A. Einstein, 69626 Villeurbanne Cédex, France

Received October 5, 1994; revised March 29, 1995

Starting from $VO(HPO_4)$, 0.5 H_2O a VPO catalyst has been activated at 400° C in an *n*-butane/air mixture. The catalyst has been characterized at different activation times (up to 132 h) by XRD, ^{31}P NMR (spin–echo mapping and magic angle spinning) and XPS. A quantitative estimation of the amount of V^{5+} has been performed in the bulk (by NMR) and on the surface (by XPS) of the catalyst. During activation, the VPO catalyst undergoes a progressive reduction (into $(VO)_2P_2O_7$) of the δ-$VOPO_4$ phase, which is also transformed in part into α_{II}-$VOPO_4$. These changes have been correlated with the evolution of the catalytic performances. The *n*-butane conversion and the selectivity for maleic anhydride increase with the V^{4+}/V^{5+} surface ratio. The results have been discussed in relation to the relevant published studies. It is concluded that the dynamic surface concentration of V^{5+} species, which are acting as oxidizing centers, is reduced during activation to a level low enough to achieve an efficient VPO catalyst. © 1995 Academic Press, Inc.

INTRODUCTION

Vanadium phosphorus oxides (VPO) are well-known catalysts for the selective oxidation of *n*-butane to maleic anhydride (MA). Though the main phase is the vanadyl pyrophosphate $(VO)_2P_2O_7$, the composition of VPO catalysts is actually complex as they also contain V^{5+} species (1–3).

Numerous questions relative to the active phase on the surface of the working catalyst are still unclear. As stated recently by Centi (4) in a critical review, the nature, amount, distribution, and evolution of V^{5+} phosphate phases during catalytic tests would require further investigations.

Most efficient VPO catalysts are generally prepared by a long-term activation of the precursor, $VO(HPO_4)$, 0.5 H_2O prepared in organic solvent under the usual reaction conditions, i.e., under *n*-butane/air flow at a temperature in the 380–450°C range.

Recent works by Volta *et al.* (5–7), using Raman spectroscopy and other techniques, and by Overbeek *et al.* (8), using DRIFTS and XRD, have pointed out the importance of studying the evolution of the catalyst in the course of the activation process. In the present work the VPO catalyst has been characterized as a function of the activation time at 400°C using XRD, BET surface area, ^{31}P NMR (MAS and spin–echo mapping), and XPS surface analysis. The current state of the catalyst has been compared with the evolution of the catalytic performances with time on stream in the *n*-butane/oxygen/helium mixture.

EXPERIMENTAL

The precursor was prepared in an organic medium (9) using *i*-butanol. V_2O_5 (11.8 g) was added to H_3PO_4 (85%), with a P/V = 1.1 atomic ratio. After refluxing (16 h) under a nitrogen flow, a light blue-green suspension was obtained and then separated by filtration. The resulting precipate was washed (with *i*-butanol and ethanol) and dried (16 h, 110°C). The XRD pattern of the precursor showed that a well-crystallized $VO(HPO_4)$, 0.5 H_2O phase was obtained (10).

Starting with the same precursor in a microreactor, four separate experiments have been done under the same flow of the reaction mixture, n-$C_4H_{10}/O_2/He$: 1.6/18/80.4 at atmospheric pressure. Note that the composition of the gas mixture was similar to the usual *n*-butane/air mixture used to activate industrial VPO catalysts. The total gas flow was 2.4 liter h^{-1} with VSHV = 1500 h^{-1}. The temperature was linearly increased (0.5°C mn^{-1}.) from room temperature up to 400°C. This initial treatment was identical for the four experiments. The difference was the time on stream at 400°C:

0.1 h	(VPO-0.1),
8 h	(VPO-8),
84 h	(VPO-84),
132 h	(VPO-132).

The catalysts were quenched after these different activation times by switching off the oven. The by-passed glass reactor cooled down rapidly to room temperature. The

0021-9517/95 $12.00

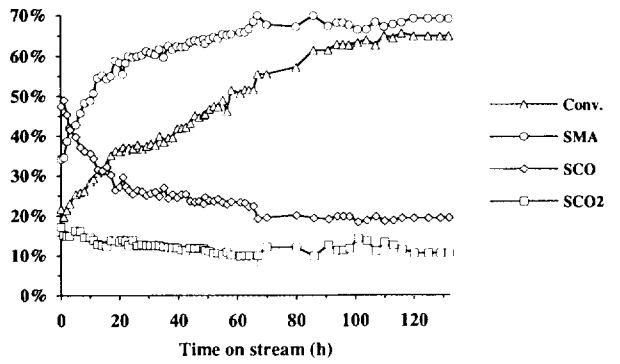

FIG. 1. Evolution of the catalytic performances with time on stream at 400°C under a mixture of n-$C_4H_{10}/H_2/He$: 1.6/18/80.4.

catalyst was then rapidly put into a small glass flask which was then filled with argon and closed.

Gas analysis was performed by on-line gas chromatography. As already described (11), hydrocarbons and oxygenates were analysed on two different columns equipped with FID detectors, CO, CO_2, H_2O, O_2, and He were analysed on a Carbosieve column with a TCD detector.

The four catalysts have been characterized by the following techniques:

— BET surface area using nitrogen adsorption at liquid nitrogen temperature.

— XRD using a Siemens D500 diffractometer with Cu$K\alpha$ radiation.

— ^{31}P NMR spin–echo mapping and magic angle spinning (MAS) on a Bruker MLS 300 spectrometer. The experimental conditions have already been described by Sananes *et al.* (12a, 12b).

— XPS in a VG ESCALAB 200 R machine using the Mg$K\alpha$ radiation. The data were collected with a DIGITAL PDS 11 computer. The electron energy analyser was operated at a pass energy of 50 eV. The charge of catalyst samples was corrected by setting the binding energy of adventitious carbon (C_{1s}) at 284.5 eV.

RESULTS

Catalytic Tests

As shown in Fig. 1, the n-butane conversion steadily increases from 20 to 65% for 132 h on stream at 400°C. The selectivity in MA also increases, first rapidly up to about 70%. We also observe a decrease in the selectivity for CO and CO_2. This is especially the case for the selectivity in CO which decreases rapidly within the first 10 h. The evolution of the conversion of n-butane and the selectivity for the main products measured for 0.1, 8, 84, and 132 h are summarized in Table 1, including also the specific activity (V_{MA}) of the formation of MA. Note that the n-butane conversion, the selectivity for MA, and V_{MA} display a similar trend; they first strongly increase with the time on stream up to 84 h and then they are nearly stabilized.

Characterization

1. BET Surfaces

We have measured the following specific areas: 10.5 m^2 g^{-1} for VPO-0.1, 7.6 m^2 g^{-1} for VPO-8, 14.7 m^2 g^{-1} for VPO-84, and 19.4 m^2 g^{-1} for VPO-132.

This evolution arises from changes in the morphology of the catalyst particles. An examination by SEM showed that VPO-0.1 and VPO-132 had the usual rose-like habit. However the individual crystallites, with a platelet shape, seem to be more split in VPO-132, in agreement with the observed increase in the surface area.

2. XRD Patterns

As shown in Fig. 2, the four VPO catalysts are very poorly crystalline. The comparison with XRD spectra of pure $(VO)_2P_2O_7$ and of the different $VOPO_4$ phases (3, 5) shows that the presence of $(VO)_2P_2O_7$ is characterized by reflections at 23°, 28.45°, and 29.94° (2Θ). Along with the pyrophosphate, the patterns indicate the additional presence of V^{5+} phases, particularly δ-$VOPO_4$ (lines at 22.08°, 28.55°, 24.16° (2Θ)). For increasing time of activation, the

TABLE 1

The Catalytic Performances of the Studied VPO Catalysts

Catalysts	Time on stream (h)	n-Butane conv. (%)	S_{MA} (%)	S_{CO} (%)	S_{CO2} (%)	$S_{Acry.}$ (%)	$S_{Acet.}$ (%)	$S_{t.But.}$ (%)	V_{MA} $\times 10^{-8}$ (mol/s.m^2)
VPO-0.1	0.1	22	34	47	17	0.3	0.2	0.4	0.43
VPO-8	8	26	48	36	15	0.5	0.1	0.3	0.99
VPO-84	84	55	66	20	12	0.6	0.2	0.1	1.48
VPO-132	132	65	69	19	11	0.6	0.2	0.1	1.39

Note. n-Butane conversion and selectivity S_i for MA (maleic anhydride), CO, CO_2, Acry. (acrylic acid), Acet. (acetic acid), t.But. (*trans*-butene); V_{MA} (specific activity of maleic anhydride formation).

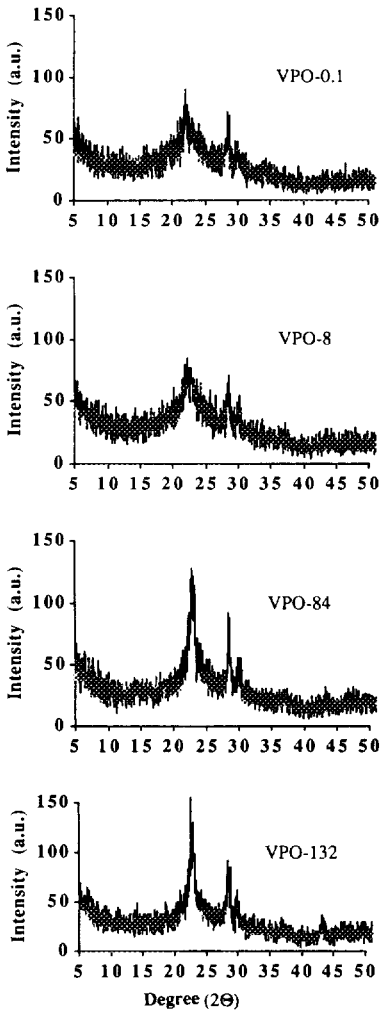

FIG. 2. XRD patterns of the studied VPO catalysts.

evolution of the XRD patterns could be interpreted as an increasing amount of $(VO)_2P_2O_7$ phase, but a crystallisation process could also explain the growth and the narrowing of the pyrophosphate lines.

3. ^{31}P NMR spectroscopy

It has already been reported (13) that the presence of paramagnetic centers in VPO catalysts drastically increased the line width and the observed frequency of ^{31}P NMR spectra. Thus, part or even the totality of the NMR information cannot be detected by standard NMR sequences, particularly when the line width is greater than the band width of the spectrometer. Li *et al.* (13) have shown that the total ^{31}P NMR spectrum could be observed using the spin–echo mapping technique. As the position of the NMR line depends on the local density of unpaired electron spin on ^{31}P nuclei, the method can be used to distinguish between various phases in the +4 vanadium oxidation state, as also shown by Sananes *et al.* (12a, 12b).

However, when V^{4+} and V^{5+} centers are simultaneously present in a material, standard ^{31}P MAS NMR can provide information about phosphorus atoms that are not perturbed by the presence of paramagnetic centers, i.e., in a V^{5+}-rich environment. In this case, the ^{31}P signal is not shifted but slightly broadened. However, chemical shift anisotropy can be partially averaged by the MAS technique, and the information is similar to that obtained on $VOPO_4$ phases.

a. Spin–echo mapping. As shown in Fig. 3, the four VPO samples give spectra with a similar general shape, showing two peaks centered at 0 ppm and at about 2400 ppm. In agreement with XRD observations, these spectra confirm that the transformation of the precursor is completed since $VO(HPO_4)$, 0.5 H_2O gives a peak at about 1750 ppm (12b). As already shown by Sananes *et al.* (12a, 12b) and Li *et al.* (13), the narrow peak at 0 ppm can be attributed to P atoms coordinated by V^{5+} cations in phosphate phases, and the broad peak near 2400 ppm can be attributed to P in the pyrophosphate phase. The maximum intensity of the latter peak has been observed at 2500 ppm by Li *et al.* (13) and at 2600 ppm by Sananes *et al.* (12a). We are presently studying the pyrophosphate phase and it appears that a large paramagnetic shift (2600 ppm) is indicative of a well-crystallised solid prepared at a high temperature (750°C). The lower shift recorded on the present samples (2400 ppm) would then agree with XRD patterns pointing to a poorly crystallised material.

The signal observed in a large region between the two peaks (500 to 1500 ppm) cannot be related to either V^{5+} phases or $(VO)_2P_2O_7$. Sananes *et al.* (12c) suggested that it could arise from the presence of V^{4+} in an amorphous matrix. In VPO materials, phosphorus tetrahedra are linked to vanadium octahedra via an oxygen atom. In these

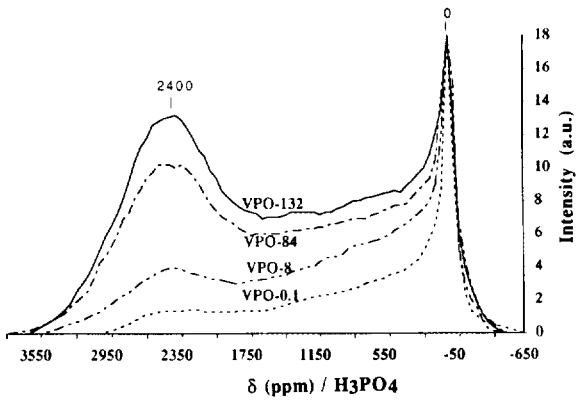

FIG. 3. ^{31}P NMR spin-echo mapping spectra of the studied VPO catalysts. (Spectra normalized with respect to the peak at 0 ppm.)

TABLE 2

^{31}P NMR Results on the Studied VPO Catalysts

Catalysts	Time on stream (h)	V^{5+} (%)	δ-$VOPO_4$ (%)	α_{II}-$VOPO_4$ (%)
VPO-0.1	0.1	39	39	0
VPO-8	8	31	25	6
VPO-84	84	22	15	7
VPO-132	132	17	10	7

Note. V^{5+} amount calculated from spectra shown in Fig. 3. Relative amount of V^{5+} phases (δ and α_{II}-$VOPO_4$) calculated from spectra shown in Fig. 4.

octahedra V atoms can be in +4 or in +5 oxidation state. Depending on that, the local density of unpaired electrons on the ^{31}P nucleus and, consequently, the NMR shift, are functions of the number of paramagnetic centers. It is therefore conceivable that upon the transformation of the hemihydrate into the pyrophosphate phase (that goes through oxidation and subsequent reduction of the precursor as shown later on), P atoms can be surrounded by 0, 1, 2, 3, or 4 V^{4+} centers, which gives a distribution of NMR shifts from about 0 to about 2500 ppm. Such an explanation appears to be also consistent with the possible presence of mixed-valence V^{4+}–V^{5+} pairs, as proposed by Lopez Granados *et al.* (14). Indeed, we did not observe any significant signal in the region 500 to 1500 ppm for a pure and well-crystallised $(VO)_2P_2O_7$ phase prepared at 750°C under nitrogen flow, from the hemihydrate precursor.

A serious question is that of the quantification of ^{31}P NMR measurements by spin–echo mapping. In fact the presence of unpaired electron spins does not alter the absolute area of ^{31}P line, but increases the line width and the observed shift. The total area is independent of the degree of vanadium reduction. Moreover, in contrast with the observed shift, the total ^{31}P NMR intensity does not change with the local environment of P atoms. A series of experiments performed on mechanical mixtures of V^{4+} and V^{5+} phases have shown that the NMR intensities were in very good agreement with those expected from chemical composition.

In the present case, the total area of the ^{31}P NMR spin–echo mapping spectrum, normalized with respect to the amount of catalyst, did not change (within the experimental error, about 10%) with activation time, providing additional evidence for the method of quantification. Note that in Fig. 3 the spectra have been normalised with respect to the V^{5+} signal at 0 ppm. Such a representation allows one to observe that the peak at 2400 ppm, typical of the crystalline $(VO)_2P_2O_7$ phase, is growing with time of activation.

A quantitative estimation of the relative V^{5+} amount has been performed by measuring the ratio between the area under the V^{5+} peak (taken as a symmetrical peak centered at 0 ppm) and the total area under the NMR spectrum. As shown in Table 2 (including also NMR-MAS results discussed below), the V^{5+} amount decreases very significantly (from 39 to 17%), from VPO-0.1 to VPO-132.

We have verified that the VPO catalyst used in this work is homogeneous at a nanometric scale using analytical electron microscopy (EDX-STEM). This observation is indeed a basic condition for the quantification.

b. M.A.S. The spectra of the four samples can be compared in Fig. 4. They are characterized by two peaks at about −11 ppm and −21 ppm. Ben Abdelouahab *et al.* (5) have presented the reference spectra of the different $VOPO_4$ phases. The δ-$VOPO_4$ phase gives a main peak at −11 ppm and a second smaller peak at about −20 ppm, whereas α_{II}-$VOPO_4$ is associated with a single peak also at about −20 ppm. Figure 4 shows a steady increase (with time of activation) of the intensity of the peak at −21 ppm with respect to the other peak at −11 ppm. There is an inversion of the relative intensity of these peaks on VPO-132 compared to VPO-0.1. Therefore the evolution of the spectra is attributed to the progressive transformation of nearly pure δ-$VOPO_4$ (on VPO-0.1) to α_{II}-$VOPO_4$.

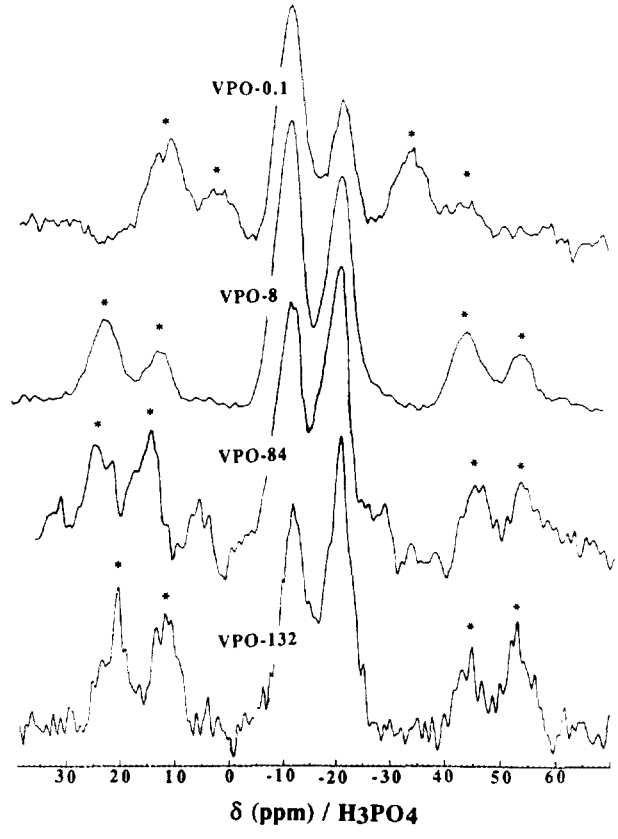

FIG. 4. ^{31}P NMR-MAS of the studied catalysts. (*) rotating bands.

TABLE 3

XPS Results on the Studied VPO Catalysts

Catalysts	Time on stream (h)	P/V	O/V	V^{4+} [516.9 eV] (%)	V^{5+} [518.0 eV] (%)
VPO-0.1	0.1	1.8	6.8	53 (1.8)	47 (1.7)
VPO-8	8	1.7	6.5	57 (1.8)	43 (1.7)
VPO-84	84	1.7	6.3	60 (1.8)	40 (1.7)
VPO-132	132	1.8	5.9	63 (1.8)	37 (1.7)

Note. Quantitative estimation of V^{4+} and V^{5+} amounts based on the decomposition of $V2p_{3/2}$ levels as shown in Fig. 5 (FWHM, in eV, are indicated in brackets.)

This transformation is not completed within 132 h; the peak at −11 ppm is still present on the spectrum recorded on VPO-132. A quantitative estimation of the δ- and α_{II}-$VOPO_4$ amounts is given on this basis in Table 2, taking into account the total V^{5+} relative concentration given by the ^{31}P NMR spin–echo mapping spectra.

4. XPS Analysis

The catalysts were briefly exposed to air in the course of their deposit on the sample holder. In preliminary experiments, we observed that air exposure at room temperature, at least for a few minutes, did not induce significant changes in the XPS results.

For quantitative analysis, the signal intensities of $V2p_{3/2}$, and O_{1s} were measured by using integrated areas under the detected peak. After smoothing the experimental spectrum, the background was subtracted using a nonlinear Shirley function. To evaluate the surface atomic ratios, we used the equation

$$n_1/n_2 = (I_{1x}/I_{2y})(\sigma_{2y} \cdot S_{2y})/(\sigma_{1x}/S_{1x}),$$

where n_1, n_2 are the number of atoms of either element 1 or element 2; I_{1x}, I_{2y} are the intensity of the peak of the core level x or y for a chosen element 1 or 2; and σ_{1x}, σ_{2y} are the cross section for X-ray excitation as calculated by Scofield (15). For our spectrometer, in a constant analyser energy (CAE) mode and at a pass energy of 50 eV, the sensitivity factors, S_{1x}, S_{2y} are proportional to $[E_k]^{0.5}$ where E_k is the kinetic energy of the emitted electrons. The experimental precision on XPS quantitative measurements is usually considered to be around 20%.

The obtained P/V and O/V atomic ratios are shown in Table 3. An excess of P and O with respect to the $(VO)_2P_2O_7$ stoichiometry is observed. With the exception of Misono *et al.* (16), a surface enrichment in phosphorus determined through XPS measurements has been also reported on V–P–O catalysts (2, 4, 17, 18, 19). This surface excess of P and O has been tentatively explained by the presence of either $VO(PO_3)_2$ (20) or pendent pyrophosphate groups (21) which provide a means for site isolation. It is also generally accepted that an excess of phosphorus on the surface stabilizes the vanadium IV oxidation state (2). Note that the P/V ratio remains constant with the time on stream (Table 3). Therefore we conclude that this important factor does not determine, at least in this work, the evolution of the V–P–O catalyst with activation time.

The relative amount of V^{4+} and V^{5+} as indicated in Table 3 has been determined by decomposition of the $V2p_{3/2}$ XPS peak. The following considerations have been used to establish the procedure of decomposition of the $V2p_{3/2}$ peak.

We have prepared a γ-$VOPO_4$ phase by calcination of the precursor $VO(HPO_4)$, 0.5 H_2O at 680°C under an air flow and also a pyrophosphate phase $(VO)_2P_2O_7$ by heating the same precursor under nitrogen flow at 750°C. DRX and ^{31}P NMR spin–echo mapping confirmed that pure γ-$VOPO_4$ and $(VO)_2P_2O_7$ have been, respectively, obtained.

As shown in Fig. 5, the measured binding energy of the $V2p_{3/2}$ level is 518.0 eV for γ-$VOPO_4$ and 516.9 eV for $(VO)_2P_2O_7$. The present measurements are in good agreement with the binding energy associated to, respectively, V^{5+} (518 to 518.2 eV) and V^{4+} (516.9 to 517.1 eV) according to Harrouch-Battis *et al.* (17), Cornaglia *et al.* (19), Moser and Schrader (22), and Bastians *et al.* (23). Indeed different values of $V2p_{3/2}$ binding energy have been

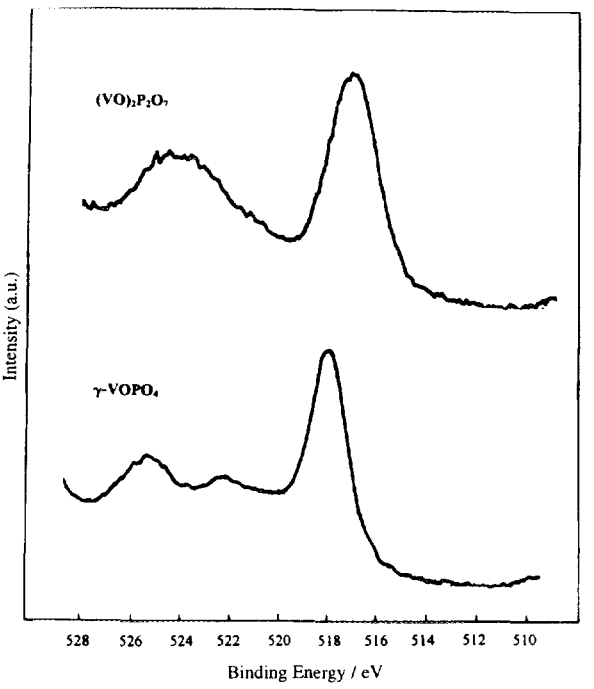

FIG. 5. XPS $V2p_{3/2}$ and $V2p_{3/2}$ levels recorded on $(VO)_2P_2O_7$ and γ-$VOPO_4$. The additional peak near 522 eV corresponds to the satellite O_{1s} peak, $MgK\alpha_{3,4}$ radiation.

also reported, ranging for V^{5+} from 518.6 (24) to 517.2 (18). Absolute values of binding energy depend on the spectrometer setting and the reference (C_{1s} at 284.5 eV in the present work). However, it may be observed that the energy difference between the V^{5+} and V^{4+} oxidation states nearly always lies in the range 1.0 to 1.2 eV. Note that the line width of the $V2p_{3/2}$ peak corresponding to V^{5+} in γ-$VOPO_4$ is narrow compared to V^{4+} in $(VO)_2P_2O_7$, as shown in Fig. 5. We are presently studying the pure pyrophosphate phase and it turns out that there is always a limited amount of V^{5+} on the surface, usually from 10 to 15%. The presence of V^{5+} is consistent with the $V2p_{3/2}$ peak being broader in $(VO)_2P_2O_7$ than in γ-$VOPO_4$.

The presence of vanadium in two oxidation states, V^{4+} and V^{5+}, on the surface of the four studied VPO can be inferred from the NMR analysis (Table 2 and Figs. 3 and 4). Indeed it would be most surprising that V^{5+} species will not be present on the surface first exposed to oxygen in the course of the activation. The fairly large $V2p_{3/2}$ peak (FWHM = 2.4 eV) of the four samples is also consistent with the presence of the two oxidation states.

The $V2p_{3/2}$ peak has been therefore decomposed into two peaks with a binding energy of 518.0 eV for V^{5+} and 516.9 eV for V^{4+}. As shown in Fig. 6, the addition of the two V^{5+} and V^{4+} spectra lead to a good fit with the experimental $V2p_{3/2}$ peak. This was carried out with a nonlinear least-squares curve-fitting program with a Gaussian/Lorentzian product function.

The evolution of the relative surface amount of V^{4+}/V^{5+} with the activation time can be directly observed in Fig. 6. As shown in Table 3, The V^{5+} amount decreases from 47% to 37% with a parallel increase in V^{4+} amount from 53% to 63%. The decrease in the O/V ratio (from 6.8 to 5.9), with no reduction of the P/V ratio, also appears to be consistent with a progressive reduction with time of the V^{5+} species.

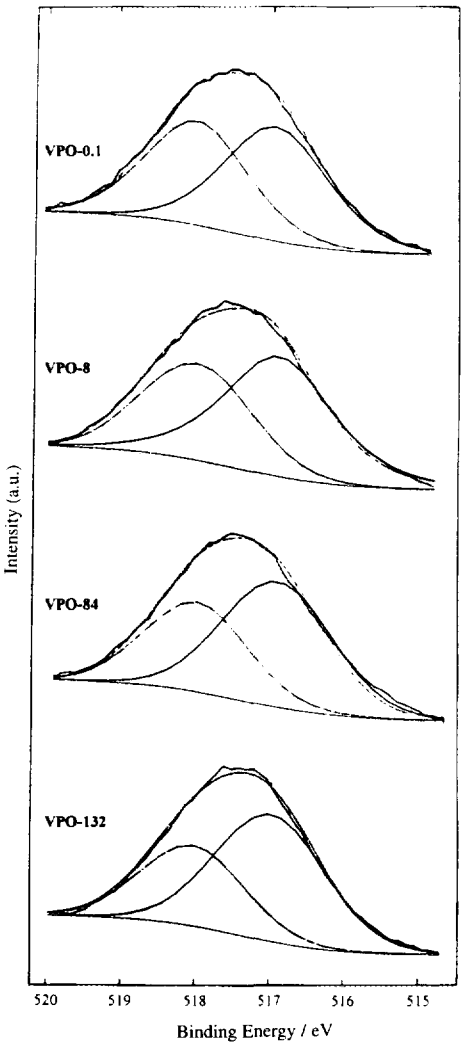

FIG. 6. Evolution with the activation of the XPS spectra of the studied catalysts showing the decomposition of the $V2p_{3/2}$ level into V^{4+} (516.9 eV) and V^{5+} (518.0 eV).

DISCUSSION

The present results show a parallelism between improving catalytic performances (*n*-butane conversion, activity, and selectivity for MA production) with activation time (Fig. 1 and Table 1) and a decrease in the amount of V^{5+} as evidenced by both NMR (Table 2) and XPS (Table 3) spectroscopies. This decrease results from a progressive reduction of V^{5+} to V^{4+} and therefore the V^{5+} domains of $VOPO_4$ are not simply redispersed. Indeed the V^{5+} amount on the surface region, as measured by XPS (Table 3), is always higher than the amount measured by ^{31}P NMR spin–echo mapping (Table 2). This observation appears to be logical as the surface of the catalyst is directly exposed to the gas-phase oxygen. There is probably a V^{5+} concentration gradient from the surface to the bulk, but the V^{5+} domains are certainly not located only on the surface; the total V^{5+} amount is much too high, especially at the beginning (39% Table 2). As calculated by Ebner *et al.* (21), the total number of V atoms should not exceed 3.4% on the surface of a catalyst with a BET surface area of 20 $m^2\ g^{-1}$ and therefore the V^{5+} concentration would be of a few percents if V^{5+} was strictly localized on the surface.

Besides a chemical reduction of V^{5+} species, a transformation of δ-$VOPO_4$ into α_{II}-$VOPO_4$ has been evidenced by ^{31}P NMR MAS (Fig. 4, Table 2). Such a phenemon has been already observed by Raman spectroscopy (5, 6) in the course of activation.

More surprising is the initial high amount of δ-$VOPO_4$ (V^{5+}) which would be formed directly from the precursor $VO(HPO_4)$, 0.5 H_2O (V^{4+}). The oxidation state of the catalyst depends on the oxidizing power of the gas phase.

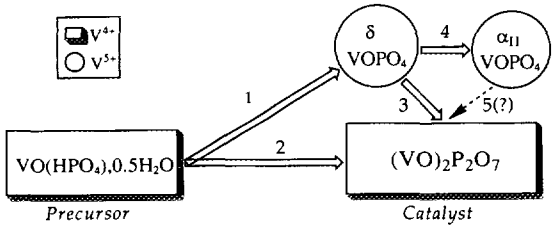

FIG. 7. Scheme of the proposed evolution of the VPO catalyst with activation time: (1) oxydehydration; (2) topotactic transformation; (3, 5) reduction V^{5+} to V^{4+}; and (4) isovalence transformation.

In the gas mixture, the O_2/n-C_4H_{10} ratio (11.3) is characterized by a large excess of O_2 with respect to the stoichiometry for *n*-butane mild oxidation (3.5) or even the combustion (5.5). We also know that the temperature of 400°C is too low to allow the oxidation of $(VO)_2P_2O_7$. We have observed that under pure oxygen, in a static apparatus, the onset of $(VO)_2P_2O_7$ surface oxidation (evidence by O_2 consumption) starts at about 530–540°C.

The precursor is not active in the mild oxidation of *n*-butane prior to its transformation through the loss of crystal water occurring around 370–380°C (7). Therefore it can be concluded that the gas mixture acts more like a simple air mixture with oxidative properties during the initial heating step, up to 400°C. It has been reported by Overbeek *et al.* (8) that $VO(HPO_4)$, 0.5 H_2O lost its crystal water and simultaneously started to oxidize at 350–380°C during the calcination in air. Above 350–380°C the reaction of *n*-butane to MA starts (7), and the conversion of butane increases with time at 400°C (Fig. 1 and Table 1). Therefore the reducing power of the gas mixture will increase accordingly with time and will provoke the progressive reduction of the V^{5+} species. Indeed such a reduction supports a redox mechanism operating in the *n*-butane oxidation reaction. Li *et al.* (13) have observed by ^{31}P NMR spin–echo mapping that V^{5+} species in $VOPO_4$, exhibiting a peak at 0 ppm, are reduced in V^{4+} species upon thermal treatment under a similar butane–air mixture. Using electrical conductivity, Rouvet *et al.* (25) have shown that all $VOPO_4$ phases are reduced when exposed to *n*-butane, δ-$VOPO_4$ being the most easily reduced.

Benabdelouahab *et al.* (26) have recently discussed the structural transformation involved in the oxydehydration of $VO(HPO_4)$, 0.5 H_2O to δ-$VOPO_4$. They also concluded that continuous coherent interfaces may be built between δ- and α_{II}-$VOPO_4$. We therefore propose the following general interpretation for the evolution of the catalysts during the activation process under *n*-butane/air mixture.

First the precursor would be in part transformed into $(VO)_2P_2O_7$ via the usually invoked topotactic process (3) and in part oxidized into δ-$VOPO_4$. Both phases are very poorly crystallized at 400°C. The activation time will mainly induce the progressive reduction of δ-$VOPO_4$ into $(VO)_2P_2O_7$ and also the transformation of δ-$VOPO_4$ into α_{II}-$VOPO_4$. This evolution of the catalysts is shown schematically in Fig. 7.

Even after 132 h on stream, it is most likely that the catalyst has not reached a complete steady state. Industrial catalysts are equilibrated only after a very long time of activation, 700 hours or more. In such equilibrated catalysts, Sananes *et al.* (12c) recently showed, by ^{31}P and ^{51}V NMR, the total absence of V^{5+} in $VOPO_4$ structure. XPS analysis on such catalysts with a decomposition of the $V2p_{3/2}$ level reveals only about 12% V^{5+}. These observations suggest that $VOPO_4$ (δ and α_{II}) remaining after 132 h of activation could be completely reduced for a longer time.

Therefore the present results also lead us to conclude that V^{5+} in the $VOPO_4$ structure is detrimental to the catalytic performances. As shown in Fig. 8, both the *n*-butane conversion and the selectivity for MA (S_{MA}) are strongly improved when the V^{4+}/V^{5+} ratio (from XPS data) increases on the surface of the catalyst. The dynamic relative amount of V^{4+} and V^{5+} on the surface of the catalyst is therefore a most important factor determining the catalytic performances.

In the mean time, the formation of CO_x decreases, especially the formation of CO. This evolution may be also correlated with the progressive reduction of the $VOPO_4$ phases as evidenced by NMR results.

The combustion of MA has been studied on $(VO)_2P_2O_7$ and $VOPO_4$ phases (11, 27–31) and it has been shown that most $VOPO_4$ phases are more active than $(VO)_2P_2O_7$. This combustion gives not only CO_2 but also CO (27, 28) according to the following reaction:

$$C_4H_2O_3 + 2\ O_2 \rightarrow 2\ CO + 2\ CO_2 + H_2O.$$

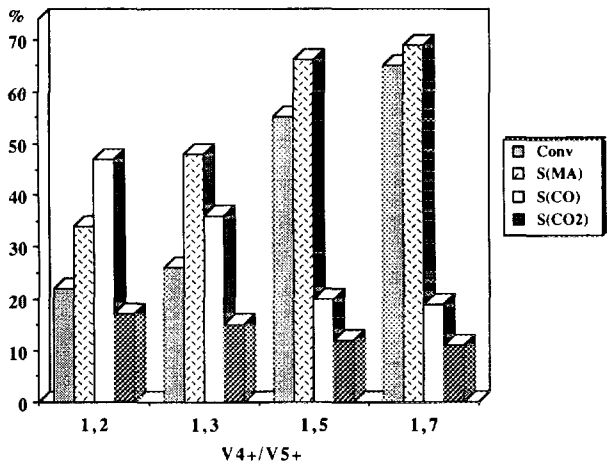

FIG. 8. Evolution of the catalytic performances as a function of the surface V^{4+}/V^{5+} ratio.

A high selectivity for CO, as initially observed (Fig. 8), can be therefore associated with the presence of V^{5+} in $VOPO_4$ phases which favour the combustion of MA as also concluded by Centi *et al.* (30).

This discussion leads to the conclusion that, on long-term equilibrated catalysts, the V^{4+}/V^{5+} ratio must be high as evidenced by the present results. As discussed by Cavani *et al.* (32), it is possible that the selectivity for MA goes through a maximum for a given degree of surface oxidation, depending on the intrinsic redox properties of the catalyst and on the experimental conditions determining the oxidizing power of the reactant mixture.

It is already known that on equilibrated catalysts, only the more or less crystallized $(VO)_2P_2O_7$ phase is usually detected (2, 4, 21) and the average oxidation state of vanadium is very close to $V_{OX} = 4$ (21). On the surface, a large number of CUS (coordinatively unsaturated sites) V^{4+} ions, acting as Lewis sites, would be required for the initial slow step of *n*-butane activation (25, 26). The presence of V^{4+} (or even V^{3+}) could also be required for dioxygen activation (31, 33). V^{5+} species are oxidizing agents with probably a conflicting dual role; active in the oxygen insertion step of the reaction (V^{5+}/V^{4+} redox couple) but also in the combustion of MA and surface intermediates. The number of surface V^{5+} ions, likely isolated as also suggested by Volta *et al.* (6), must be small enough, adapted to the steady-state concentration of activated *n*-butane molecules (much less reactive than butenes or butadiene). Indeed the steady state of the catalyst will also depend on the oxidation rate of V^{4+} ions, the stability of which towards oxidation would be increased on the equilibrated VPO catalyst (2). The oxidizing power of V^{5+} species would not depend only on their total concentration but also on their local surface distribution. As recently proposed by Grasselli *et al.* (34), active sites composed of four vanadium dimers would be isolated by an excess of phosphorus in the form of pyrophosphate groups (21, 34), preventing the diffusion of excess oxygen from neighbouring sites (34).

CONCLUSION

VPO catalysts giving the best yields in MA are usually prepared by a long-term activation under an *n*-butane/air mixture. Deeper insight into the physicochemical changes occuring during the activation should yield significant clues relative to the surface state and the active sites of the working catalyst. This prompted us to gain quantitative information on the amount of V^{5+} species within the bulk and on the surface, and on the nature and evolution of $VOPO_4$ phases as function of time on stream at 400°C, under an *n*-butane/air mixture. On the basis of mainly ^{31}P NMR and XPS measurements, it has been shown that the precursor $VO(HPO_4), 0.5\ H_2O$ is first partially transformed into $(VO)_2P_2O_7$ and partially oxidized into δ-$VOPO_4$. Both phases are very poorly crystallized. Note also that δ-$VOPO_4$ cannot be localised as only small domains on the surface, its total amount being too high (about 39%), as measured by ^{31}P NMR spin–echo mapping. Then the catalyst undergoes a slow reduction with a significant decrease of the amount of $VOPO_4(V^{5+})$; δ-$VOPO_4$ is reduced in part to $(VO)_2P_2O_7$ and in part transformed into α_{II}-$VOPO_4$.

These transformations have been correlated with the improvement of the *n*-butane conversion (from 22 to 65%) and of the selectivity for MA (from 34% to 69%) with time on stream (up to 132 h). It has been shown that the catalytic performances increase with the V^{4+}/V^{5+} surface ratio, as measured by XPS.

The results have been discussed in relation to the relevant previous published works. It is proposed that $VOPO_4$ phases would be detrimental because they favour the combustion reactions. However, a small enough number of V^{5+}, probably isolated on a $(VO)_2P_2O_7$ matrix, would be required for oxygen insertion into the hydrocarbon intermediates according to a redox mechanism.

ACKNOWLEDGMENTS

We thank Dr. J.C. Vedrine and Dr. J.C. Volta for valuable comments and discussions.

REFERENCES

1. Hodnett, B. K., *Catal. Rev. Sci. Eng.* **27,** 373 (1986); *Catal. Today* **1,** 477 (1987).
2. Centi, G., Trifirò, F., Ebner, J. R., and Francheti, J. M., *Chem. Rev.* **88,** 55 (1988).
3. Bordes, E., *Catal. Today,* **1,** 499 (1977).
4. Centi, G., *Catal. Today* **16,** 5 (1993).
5. Ben Abdelouahab, F., Olier, R., Guilhaume, N., Lefevre F., and Volta, J. C., *J. Catal.* **134,** 151 (1992).
6. Volta, J. C., Bere, K., Zhang, Y. J., and Olier, R., *in* "Catalytic Selective Oxidation" (S. T. Oyama and J. W. Hightower, Eds), ACS Symposium Series, Vol. 523, p. 217, 1993.
7. Hutchings, G. J., Desmartin-Chamel, A., Olier, O., and Volta, J. C., *Nature* **348,** 41 (1994).
8. Overbeek, R. A., Versluijs-Helder, M., Warringa, P. A., Bosna, E. J., and Geus, J. W., *in* "New developements in Selective Oxidation Studies in Surface Sci. and Catal." (V. Cortès Corberán and S. Vic Bellòn, Eds.), Vol. 82, p. 183, 1994.
9. Yang, T. C., Rao, K. K., Der Huang, I., and Exxon Res. Eng. Co., U.S. Patent 4,392,986 (1987).
10. Torardi, C. C., Calabrese, J. C., *Inorg. Chem.* **23,** 1308 (1984).
11. Zhang-Lin, Y., Forissier, M., Sneeden, R. P., Védrine, J. C., and Volta, J. C., *J. Catal.* **145,** 256 (1994).
12. (a) Sananes, M. T., Tuel, A., and Volta, J. C., *J. Catal.* **145,** 251 (1994); (b) Sananes, M. T., Tuel, A., Hutchings, G. J., and Volta, J. C., *J. Catal.* **148,** 395 (1994); (c) Sananes, M. T., Bortinger, A., Vedrine, J. C., and Volta, J. C., submitted.
13. Li, J., Lashier, M. E., Schrader, G. L., and Gerstein, B. C., *Appl. Catal.* **73,** 83 (1991).
14. Lopez Granados, M., Conesa, J. C., and Fernànez-Garcìa, M., *J. Catal.* **141,** 671 (1993).
15. Scofield, J. H., *J. Electron Spectrosc.* **8,** 129 (1976).
16. Okuhara, T., Nakama, T., and Misono, M., *Chem. Lett.,* 1941 (1990).

17. Harrouch Batis, N., Batis, H., Ghorbel, A., Vedrine, J. C., and Volta, J. C., *J. Catal.* **128,** 248 (1991).
18. Garbassi, F., Bart, J., Tassinari, R., Vlaic, G., and Labarde, P., *J. Catal.* **98,** 317 (1986).
19. Cornaglia, L. M., Caspani, C., and Lombardo, E. A., *Appl. Catal.* **74,** 15 (1991).
20. Mutsuura, I., and Yamazaki, M., *in* "New Developments in Selective Oxidation" (G. Centi and F. Trifirò, Eds.), Stud. Surf Sci. Vol. 55, p. 563. Elsevier, Amsterdam, 1990.
21. Ebner, J. R., and Thompson, M. R., *Catal. Today* **16,** 51 (1993).
22. Moser, T. P., and Schrader, G. L., *J. Catal.* **104,** 99 (1987).
23. Bastians, Ph., Genet, M., Daza, L., Acosta, D., Ruiz P., and Delmon, B., *in* "New Developments in Selective Oxidation by Heterogeneous Catalysis, Studies in Surface Sci. and Catal." (P. Ruiz and J. B. Delmon, Eds), Vol. 72, pp. 267–278. Elsevier, Amsterdam 1992.
24. Zazhigalov, V. A., Belousov, V. M., Komashko, G., Pyanitskaya, A. I., Merkureva, Y. N., Poznyakevich, A. L., Stoch, J., and Haber, J., "Proceedings, 9th International Congress on Catalysis, Calgary, 1988" (M. J. Phillips and M. Ternan Eds.), Vol. 4, p. 1546. Chem. Institute of Canada, Ottawa, 1988.
25. Rouvet, F., Hermann, J. M., and Volta, J. C., *J. Chem. Soc. Faraday Trans.* **90,** 1441 (1994).
26. Benabdelouahab, F., Volta, J. C., and Olier, R., *J. Catal.* **148,** 334 (1994).
27. Zazhigalov, V. A., Zaytsev, Y. P., *Katal. Katal.* **20,** 51 (1987).
28. Moser, T. P., Wenig, R. W., and Schrader, G. L., *Appl. Catal.* **34,** 39 (1987).
29. Szakàcs, S., Wolf, H., Mink, G., and Bertòti, I., *Catal. Today* **1,** 27 (1987).
30. Centi, G., Trifirò, F., Busca, G., J. Ebner, J., and Gleaves, J., *Faraday Discuss. Chem. Soc.* **87,** 215 (1989).
31. Busca, G., Centi, G., and Trifirò, F., *Appl. Catal.* **25,** 265 (1989).
32. Cavani, G., Centi, G., Trifirò, F., and Grasselli, R. K., *Catal. Today* **3,** 185 (1988).
33. Bordes, E., *Catal. Today,* **16,** 27 (1993).
34. Agaskar, P. A., DeCaul, L., and Grasselli, R. K., *Catal. Today* **23,** 339 (1994).